[CANCER RESEARCH 64, 1359–1368, February 15, 2004]

Acquisition of High-Level Chromosomal Instability Is Associated with Integration of Human Papillomavirus Type 16 in Cervical Keratinocytes

Mark R. Pett,[1] William O. F. Alazawi,[1] Ian Roberts,[1] Sally Dowen,[4] David I. Smith,[3] Margaret A. Stanley,[2] and Nicholas Coleman[1,2]

[1]Medical Research Council Cancer Cell Unit, MRC/Hutchison Research Centre, and [2]Department of Pathology, University of Cambridge, Cambridge, United Kingdom; [3]Department of Experimental Pathology, Mayo Clinic, Rochester, Minnesota; and [4]Molecular Oncology Unit, Cancer Research UK, Hammersmith Site, London, United Kingdom

ABSTRACT

Whereas two key steps in cervical carcinogenesis are integration of high-risk human papillomavirus (HR-HPV) and acquisition of an unstable host genome, the temporal association between these events is poorly understood. Chromosomal instability is induced when HR-HPV E7 oncoprotein is overexpressed from heterologous promoters *in vitro*. However, it is not known whether such events occur at the "physiologically" elevated levels of E7 produced by deregulation of the homologous HR-HPV promoter after integration. Indeed, an alternative possibility is that integration *in vivo* is favored in an already unstable host genome. We have addressed these issues using the unique human papillomavirus (HPV) 16-containing cervical keratinocyte cell line W12, which was derived from a low-grade squamous intraepithelial lesion and thus acquired HPV16 by "natural" infection. Whereas W12 at low passage contains HPV16 episomes only, long-term culture results in the emergence of cells containing integrated HPV16 only. We show that integration of HPV16 in W12 is associated with 3′ deletion of the E2 transcriptional repressor, resulting in deregulation of the homologous promoter of the integrant and an increase in E7 protein levels. We further demonstrate that high-level chromosomal instability develops in W12 only after integration and that the forms of instability observed correlate with the physical state of HPV16 DNA and the level of E7 protein. Whereas intermediate E7 levels are associated with numerical chromosomal abnormalities, maximal levels are associated with both numerical and structural aberrations. HR-HPV integration is likely to be a critical event in cervical carcinogenesis, preceding the development of chromosomal abnormalities that drive malignant progression.

INTRODUCTION

Infection by high-risk human papillomaviruses (HR-HPVs) is a necessary cause of cervical carcinoma (1). The majority of cases are squamous cell carcinomas (SCCs), which arise in a multistep fashion from precursor squamous intraepithelial lesions (SILs; Ref. 2). The major transforming and immortalizing proteins of HR-HPVs, such as human papillomavirus (HPV) 16 and HPV18 (3), are E6 and E7, which bind and inactivate p53 and pRB, respectively (4, 5). In productive infections, E6 and E7 expression is confined to the postmitotic suprabasal cells of the squamous epithelium (6, 7) and appears to be repressed by host factors within basal dividing cells (8). In contrast, in neoplastic lesions (high-grade SIL and SCC), the viral oncogenes are expressed in the basal layers (7).

Deregulation of the HPV early promoter is therefore an important early event in cervical carcinogenesis. Whereas such deregulation may reflect altered host control over the HPV early promoter (4), an important alternative cause is integration of HR-HPV into the host genome. Integration usually causes deletion or disruption of the E2 repressor of early gene transcription (9), which in turn leads to increased levels of the E7 protein and acquisition of a growth advantage (10, 11). Virtually all HPV16/18-positive cervical carcinomas contain integrated viral genomes from which early genes are transcribed (12), suggesting that integration plays an important role in cervical carcinogenesis *in vivo*.

Although necessary, deregulation of HR-HPV E6 and E7 expression is insufficient for development of the malignant phenotype. Genomic instability, producing specific genomic aberrations, is also associated with the development and progression of cervical carcinomas (13–16). The temporal relationship between integration of HR-HPV and acquisition of a genetically unstable environment has not previously been demonstrated. High levels of HR-HPV E7 and E6, as expressed from heterologous promoters *in vitro*, can induce genomic instability (17, 18). HR-HPV integration *in vivo* may therefore promote high-level genomic instability via increased levels of the viral oncoproteins caused by deregulation of the homologous HR-HPV promoter. Conversely, integration may be favored in an already chromosomally unstable environment, perhaps related to deregulated host control over viral early gene expression (4, 19).

Investigation of the temporal relationship between HR-HPV integration and host genomic instability has previously been difficult due to the lack of a suitable model system. Here, we present results from W12, a unique cervical keratinocyte cell line infected with HPV16, the HPV type most commonly found in cervical SCC (20). W12 was established from a low-grade SIL and thus arose by "natural" cervical infection with HPV *in vivo* (21). At early passages, W12 is diploid and maintains HPV16 episomes at approximately 100 copies/cell (10, 21). Furthermore, it recapitulates the histological characteristics of the low-grade lesion from which it was derived when grafted onto the flank of a nude mouse. As shown previously by our group, integration of viral episomes is observed during long-term *in vitro* cultivation of polyclonal W12 (10).

Here, we show that the increased levels of E7 protein seen in W12 in monolayer culture after integration are associated with deletion of the 3′ region of the E2 open reading frame (ORF), resulting in deregulation of the homologous HPV16 promoter. W12 in monolayer culture therefore represents an accurate model of events that occur in the basal cells of the cervical epithelium *in vivo*. We demonstrate that W12 cells containing HPV16 episomes are diploid and generally chromosomally stable, with only a low frequency of tetraploid cells. In contrast, HPV16 integration is associated with the acquisition of genomic abnormalities, the types of which correlate with the physical state of the HPV16 DNA and the level of E7 protein. We also describe detailed mapping of the HPV16 integration site in W12 and demonstrate that W12, after HPV16 integration, shows increased colony-forming efficiency (CFE) and reforms a higher-grade epithelium in organotypic culture, compared with passages in which only HPV16 episomes are present. Our data further indicate that the W12 cell line is a valuable reagent for studying the biology of HPV16-associated cervical carcinogenesis.

MATERIALS AND METHODS

Cell Culture. The cells used were as follows: normal ectocervical keratinocytes obtained after hysterectomy for disease unrelated to the cervix; W12 between passage 9 (W12p9) and passage 55 (W12p55); and the cervical SCC

Received 10/13/03; revised 11/18/03; accepted 12/2/03.

Grant support: Medical Research Council.

The costs of publication of this article were defrayed in part by the payment of page charges. This article must therefore be hereby marked *advertisement* in accordance with 18 U.S.C. Section 1734 solely to indicate this fact.

Requests for reprints: Nicholas Coleman, Medical Research Council Cancer Cell Unit, MRC/Hutchison Research Centre, Hills Road, Cambridge CB2 2XZ, United Kingdom. Phone: 44-1223-763285; Fax: 44-1223-763284; E-mail: nc109@cam.ac.uk.

cell lines SiHa (22) and CaSki (23). Cells were cultured as described in detail elsewhere (21, 24). All cells were passaged to approximately 90% confluence, with cells undergoing approximately 4–5 population doublings/passage. Metaphases for cytogenetic analysis were prepared from cells in monolayer culture by hypotonic lysis in KCl (25). To determine CFE, W12 cells were seeded in triplicate at densities of 100 and 500 viable cells/50-mm dish in the presence of 5×10^5 lethally irradiated murine 3T3 J2 feeder cells. When colonies were visible, feeders were removed, and colonies were stained in 0.1% toluidine blue. Percentage of CFE was determined as follows: (number of colonies/number of cells seeded) $\times$ 100 (26).

Organotypic Raft Culture. Collagen rafts incorporating mouse dermal papilla cells were prepared in 24-well plates, as described in detail elsewhere (24). Keratinocytes (1×10^5) were seeded onto each raft, and the rafts were subsequently raised to an air:liquid interface for 9–12 days. After formalin fixation, rafts were processed to paraffin for histological analysis.

Southern Analysis of Physical State of HPV16. Genomic DNA (gDNA) was prepared from cells in monolayer culture as described previously (10). A total of 5–10 μg of gDNA was restriction enzyme digested, electrophoresed through a 0.8% agarose gel, and transferred to a Hybond-N+ nylon membrane for subsequent hybridization. The restriction enzymes used were *Hin*dIII, *Bam*HI, *Nco*I, *Sda*I, *Eco*RI, and *Pst*I. Probe was prepared by excision of full-length HPV16 DNA from the pspHPV16 plasmid (21), followed by labeling with [α-^{32}P]dCTP by random priming.

PCR for the HPV16 E2 ORF. The gDNA was amplified using primer pairs specific to the HPV16 E2 ORF. Primer sets 1, 2, and 3 amplified between nucleotides 2755 and 3321, 3453 and 3714, and 2755 and 3852 of the HPV16 genome (National Center for Biotechnology Information accession number NC001526), respectively. Details of all primer sets have been given elsewhere (10, 27, 28). Cycling conditions were 94°C for 4 min; followed by 30 cycles of 94°C for 1 min, 58°C for 1 min, and 72°C for 1 min; followed by 10 min at 72°C. Products were electrophoresed on a 1% agarose gel. The expected product sizes for primers pairs 1, 2, and 3 were 567, 262, and 1122 bp, respectively. The increase in size of the product for primer pair 3 was due to the presence of linker sequences (10).

Restriction Site-PCR (RS-PCR). RS-PCR enables amplification of unknown nucleotide sequences adjacent to known nucleotide sequences (29). The use of RS-PCR to generate PCR products spanning HR-HPV host junction fragments in cervical carcinomas has been described previously (30). A total of 50 ng of gDNA from W12p55 was amplified with various combinations of HPV16-specific and restriction site oligonucleotide primers using low stringency cycling conditions, followed by a high stringency nested PCR. PCR products were then sequenced using the appropriate HPV16-specific sequencing primers. All primers and PCR conditions were as described previously (30).

Comparative Genomic Hybridization (CGH). CGH was performed as described previously (31). Test gDNA and normal male reference gDNA were labeled by nick translation with Spectrum Green-dUTP (Vysis) and Spectrum Red-dUTP (Vysis), respectively. Probe comprising 300 ng of test DNA, 300 ng of reference DNA, and 15 μg of human Cot-1 DNA (Roche) was hybridized to cytogenetically normal male metaphases (Vysis). After hybridization, signal from Spectrum Green-dUTP was enhanced with a single antibody detection using anti-fluorescein rabbit IgG fraction Alexa Fluor 488 conjugate (Molecular Probes). Chromosomes were counterstained with 4′,6-diamidino-2-phenylindole (DAPI)/antifade solution (Vector Laboratories). Images for CGH analysis were sequentially captured using an Axioplan II epifluorescence microscope (Zeiss) equipped with a Sensys charge-coupled device camera (Photometrics) and appropriate filters (Chroma Technology). The system was controlled by SmartCaptureVP Software (Digital Scientific). At least 10 metaphases for each sample were then analyzed using QUIPS XL software (Vysis). The thresholds used for detection of loss and gain were 0.85 and 1.15, respectively, with a ratio of >1.5 denoting high-level copy number gain (amplification). Reference DNA from normal male placenta was used to provide an internal sex-mismatched control for each hybridization. This meant that copy number imbalances (CNIs) on the X chromosome could not be detected.

Spectral Karyotyping. Spectral karyotyping analysis was carried out as described previously (25), using the 24-color SkyPaint probe mixture supplied by Applied Spectral Imaging. Spectral images were captured using a Nikon Eclipse E800 epifluorescence microscope equipped with a SD200 SpectraCube system (Applied Spectral Imaging). At least 10 raw spectral image files were acquired for each sample using Spectral Imaging version 2.3 software (Applied Spectral Imaging) and analyzed using SkyView version 1.6.1 software (Applied Spectral Imaging). Inverted DAPI images were used to map breakpoints of structural rearrangements.

Chromosome-Specific and Band-Specific Painting. Whole chromosome paint for chromosome 3 was prepared by degenerate oligonucleotide-primed PCR from flow-sorted chromosomes and labeled with digoxigenin-11-dUTP (Roche), as described previously (25). After overnight hybridization, probe was detected using anti-digoxigenin FITC-conjugated Fab fragments (Roche). Band-specific probes for 5p15, 5p14, 5p11–12, and 3q21 (Research Genetics) were prepared and labeled with biotin-16-dUTP (Roche), digoxigenin-11-dUTP, or Spectrum Orange-dUTP (Vysis), as described previously (25). Band-specific probes were hybridized overnight in combination with other differentially labeled band-specific probes or whole chromosome paints, as required. Biotin-16-dUTP and digoxigenin-11-dUTP were detected using avidin-Cy5 (Amersham) and anti-digoxigenin FITC-conjugated Fab fragments (Roche), respectively. For both chromosome-specific and band-specific paints, metaphases were counterstained with DAPI/antifade, and imaging was performed using the epifluorescence microscope system, as described for CGH analysis.

HPV16 Fluorescence *in Situ* Hybridization. Full-length HPV16 DNA (1 μg) from the pspHPV16 plasmid (21) was labeled by nick translation with biotin-16-dUTP. Probe comprising 100 ng of labeled HPV16 and 3 μg of Cot-1 carrier DNA was hybridized to W12 metaphase chromosomes for 2 days under the same conditions used for band-specific painting (25). After hybridization, signal was detected using three layers, streptavidin-fluorolink Cy3 (Amersham) followed by biotinylated anti-avidin D (Vector Laboratories) and then streptavidin-fluorolink Cy3. Metaphases were counterstained with DAPI/antifade and analyzed as described above.

RESULTS

The polyclonal W12 cell line has been subjected to long-term *in vitro* culture in our laboratories (Table 1), and we have previously

Table 1 *Properties of W12 in long-term tissue culture*

W12 passage	HPV16 copy no.[a]	Physical state of HPV16 genomes[b]	E7 protein level[c]	E2 expression[d]	Telomerase activity[e]	% CFE[f]	
						100 cells	500 cells
9	100	Episomal	Low	Positive	Positive	9.3 ± 1.8	9.4 ± 0.5
14	30	Episomal & integrated	Intermediate	Negative	Positive	24.0 ± 1.0	21.2 ± 0.7
24	10	Integrated	High	Negative	Positive	38.7 ± 1.9	33.7 ± 0.8
34	10	Integrated	High	Negative	Positive	43.3 ± 1.9	35.7 ± 2.2
44	10	Integrated	High	Negative	Positive	56.0 ± 1.5	47.7 ± 0.6
55	10	Integrated	High	Negative	Positive	47.7 ± 5.8	40.1 ± 1.2

[a] Number of HPV16 genome copies per cell, as estimated by Southern blot using copy number reconstructions (10). HPV, human papillomavirus.
[b] Episomal HPV16 genomes were present in both monomeric and multimeric forms. The emergent viral integration event had a type 1 pattern similar to that observed in SiHa (10, 11).
[c] Determined by Western blot (10).
[d] Determined by reverse transcription-PCR for full-length HPV16 E2 mRNA (10).
[e] Telomerase activity in protein extracts was determined by the telomeric repeat amplification protocol assay and was comparable at all passages analyzed (data not shown).
[f] Numbers represent the percentage of viable cells plated that gave rise to colonies 14 days after plating. CFE, colony-forming efficiency. Values shown are the mean % CFE ± SE calculated for three independent platings.

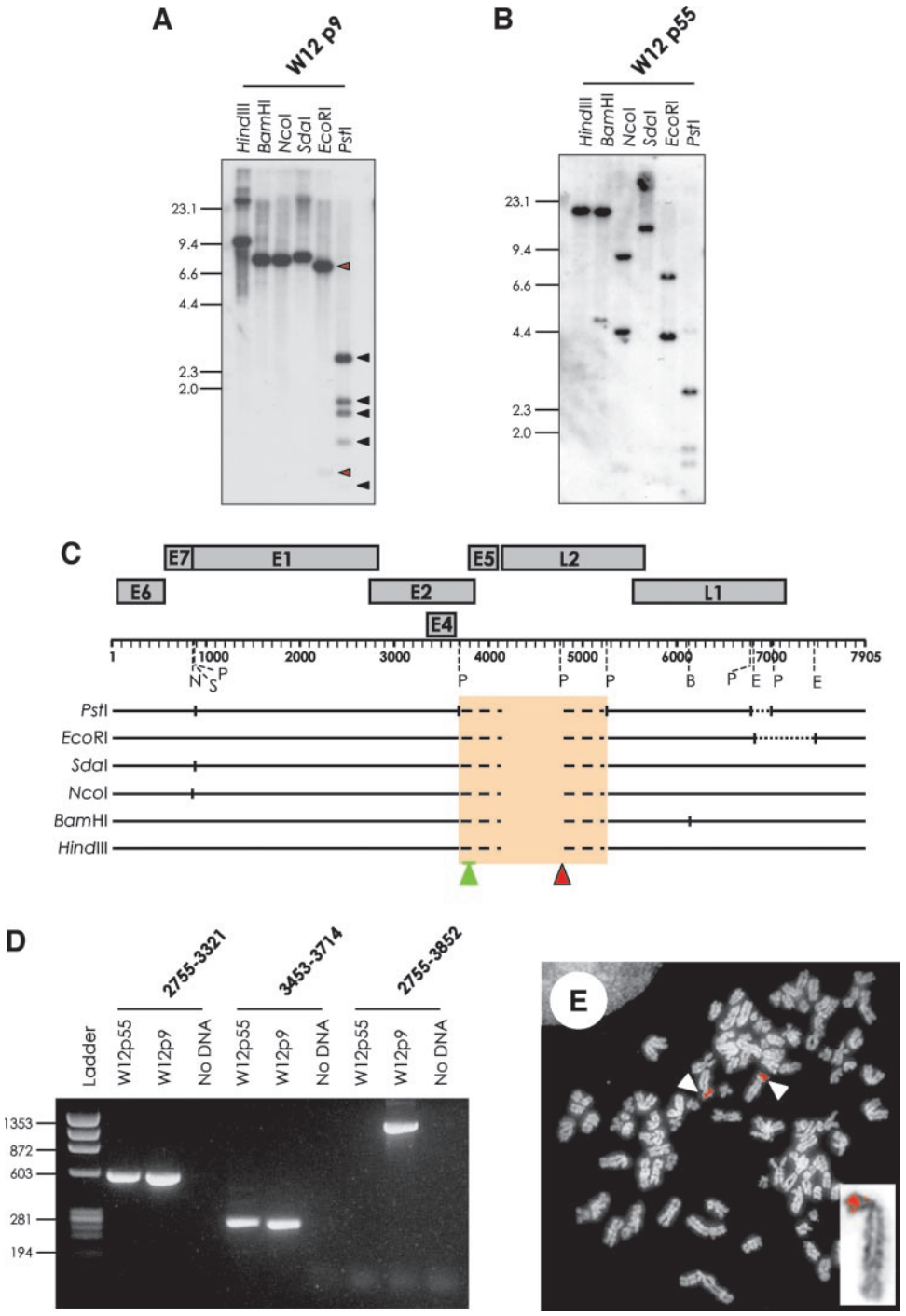

Fig. 1. Southern analysis of the physical state of human papillomavirus (HPV) 16 in W12. *A* and *B*, gDNA from W12p9 and W12p55 in monolayer culture was digested with the restriction enzymes shown. For W12p9, the sizes of the expected fragments after *Eco*RI (*red arrows*) and *Pst*I (*black arrows*) digestion of unit-length monomeric HPV16 episomes are indicated. The smallest fragment generated by the *Pst*I digestion (216 bp) could not be resolved. *C*, schematic representation of the HPV16 integration pattern in W12p55, as determined by Southern analysis. Positions of restriction sites for *Bam*HI (*B*), *Nco*I (*N*), *Sda*I (*S*), *Eco*RI (*E*), and *Pst*I (*P*) in the HPV16 genome are indicated. The *solid lines* shown *below* represent HPV16 fragments generated after digestion with the respective restriction enzyme. *Dotted lines* (for *Pst*I and *Eco*RI) indicate low molecular weight fragments that could not be detected by Southern analysis but which, given the overall banding pattern, were likely to be present. Virus-host junctions were localized to within the *colored box*, although accurate identification of the viral breakpoints was not possible using Southern analysis, as indicated by the *dashed lines*. The *red arrow* indicates the precise region of the upstream breakpoint, as determined by RS-PCR, and the *green arrow* and *bar* indicate the region of the downstream breakpoint, as determined by E2 PCR. *D*, E2 PCR analysis of W12p9 and W12p55. In W12p55, there is an absence of a product amplifying between nucleotides 2755 and 3852 but the presence of a product amplifying between nucleotides 3453 and 3714. *E*, HPV16 fluorescence *in situ* hybridization detection of integrated HPV16 (*red*; *arrowed*) in two apparently identical copies of chromosome 5 (*inset*) in W12p55.

described a limited Southern analysis of the physical state of HPV16 (10). At early passages, W12 contains approximately 100 HPV16 episomes per cell, which are stably maintained. In the passage series investigated previously (and also used in the current study), integration commenced at passage 14 and was associated with rapid loss of episomes and the emergence of a population of cells with approximately 10 copies of a single HPV16 integration site. The integrated HPV16 DNA was stably maintained thereafter. Integration was associated with loss of transcription of HPV16 E2 and increased expression of the HPV16 E7 protein (10). All passages analyzed demonstrated telomerase activity, as assessed by the telomeric repeat amplification protocol assay (data not shown). These features of the W12 series analyzed in the present study are summarized in Table 1.

Confirmation That HPV16 in W12p9 Is Exclusively Episomal. To confirm that W12p9 contained exclusively episomal HPV16, Southern analysis was performed using a large panel of restriction enzymes (Fig. 1*A*). Digestion with *Hin*dIII (a HPV16 non-cutter) produced a banding pattern consistent with the presence of both monomeric and multimeric episomal HPV16 (10). Digestion with *Bam*HI, *Nco*I, and *Sda*I (all HPV16 single cutters) each produced a prominent band of 7.9 kb, representing full-length linearized HPV16 episomes. Digestion with the HPV16 multi-cutters *Eco*RI (two cuts) and *Pst*I (six cuts) generated only the prototype bands expected from digestion of episomal HPV16 DNA. Additional bands indicative of virus-host junctional fragments were absent. The data from all restriction enzymes used indicated that W12p9 contained episomal HPV16 only.

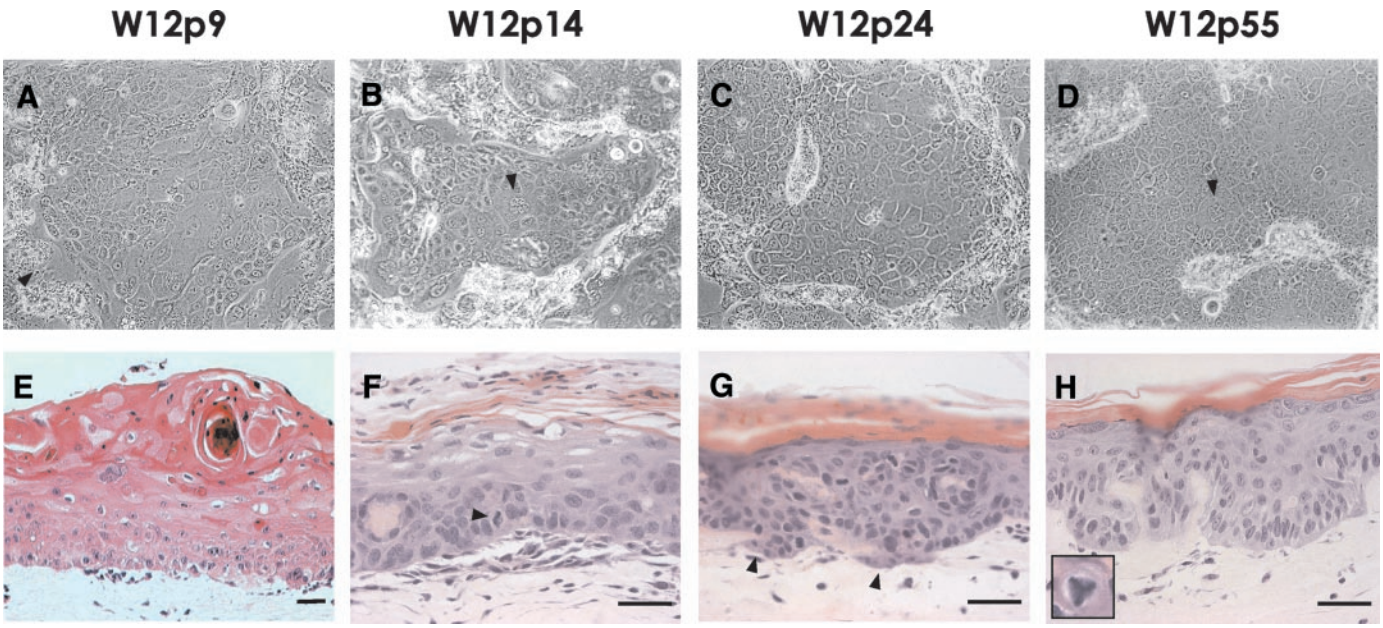

Fig. 2. Morphological characteristics of W12 in submerged monolayer culture and histological features in organotypic raft culture. Appearances of colonies in monolayer tissue culture (*A*−*D*; phase-contrast microscopy; original magnification, ×100) and of epithelium reconstituted in organotypic culture (*E*−*H*; H&E stained; *scale bar* = 50 μM) are shown for W12p9 (*A* and *E*), W12p14 (*B* and *F*), W12p24 (*C* and *G*), and W12p55 (*D* and *H*). *Arrowheads*: *A*, lethally irradiated fibroblast cells; *B* and *D*, multinucleated cells; *F*, mitotic figure in the basal layer of the W12p14 epithelium; *G*, irregular islands of basal cells infiltrating the underlying collagen matrix. *Inset* in *H*, an abnormal tripolar mitotic figure from the middle third of the W12p55 epithelium elsewhere in the raft.

Disruption of the HPV16 Genome after Integration. To determine the region of HPV16 deleted during integration, the same panel of restriction enzymes was used in Southern analysis of W12p55 (Fig. 1*B*). Bands indicating the presence of HPV16 episomes were not seen. The detection of two bands after restriction with *Bam*HI, *Nco*I, and *Sda*I indicated that the single restriction sites for each enzyme (see Fig. 1*C*) were retained in the integrated HPV16 DNA. After digestion with the HPV16 multi-cutter *Pst*I, the absence of the prototype bands spanning E5, the 3′ region of E2, and most of L2 suggested that the viral breakpoints at the two virus-host junctions were within this region (Fig. 1*C*).

Virus-Host Junction Breakpoint Mapping by RS-PCR, E2 PCR, and HPV16 Fluorescence *in Situ* Hybridization. Detailed mapping of virus-host junctions was performed on W12p55 gDNA using RS-PCR (29, 30, 32). A PCR product comprising the upstream virus-host junction was generated (data not shown). The viral DNA breakpoint was at nucleotide 4791 of the L2 ORF, consistent with predictions from Southern analysis (Fig. 1*C*). A RS-PCR product comprising the downstream virus-host junction was not generated.

PCR analysis showed absence of the full-length HPV16 E2 ORF in W12p55 (Fig. 1*D*), consistent with the absence of the full-length E2 transcript in W12p55 that we have described previously (10). In contrast, the full-length HPV16 E6 and E7 ORFs were detected in W12p55 by PCR (data not shown). We concluded that the second (downstream) virus-host junction in W12p55 was located at the 3′ region of the E2 ORF, between nucleotides 3715 and 3852 of the HPV16 genome (Fig. 1*C*). Taken together, these results demonstrated that the selected HPV16 integrant in high-passage W12 showed disruption of the E2, E5, and L2 ORFs.

A search for the host cell sequences in the RS-PCR product using the National Center for Biotechnology Information BLAST database revealed that the HPV16 DNA was integrated at chromosome band 5p15.1, which also contains the common fragile site FRA5E. Consistent with this data, HPV16 fluorescence *in situ* hybridization on metaphases of W12p55 showed integrated HPV16 at the distal p arm of two identical chromosomes (Fig. 1*E*) that were shown by enhanced inverse DAPI banding to be normal copies of chromosome 5.

Using the sequence of the RS-PCR product, we designed PCR primers spanning the upstream virus-host junction. Whereas an appropriately sized band was generated for W12p55, there was no band for W12p9 (data not shown). We concluded that because the integrant detectable in W12p55 was not seen in W12p9 at the limits of sensitivity of PCR, it arose from a true *de novo* integration event, rather than through *in vitro* selection of a rare clone containing integrated HPV16.

Progression of W12 *in Vitro* Is Associated with Acquisition of a Growth Advantage. During the transition from the presence of purely episomal to fully integrated HPV16, there was a progressive increase in the CFE of W12 in monolayer culture (Table 1). The CFE of W12p24 (integrated HPV16 only) was 3–4-fold higher than that of W12p9 (episomal HPV16 only). Further increases in CFE were also observed at passages higher than passage 24, suggesting that additional changes may have been acquired by W12 after HPV16 integration, resulting in a further selective growth advantage in monolayer culture.

Morphology of W12 in Monolayer Tissue Culture. Similar to normal ectocervical cells in monolayer culture (33), colonies of W12p9 comprised a heterogeneous population showing some evidence of stratification and differentiation (Fig. 2*A*). The features of W12p14 (Fig. 2*B*) were similar, except that multinucleate cells were frequently observed at the center of colonies. In contrast, in W12p24 and higher passages, colonies contained a relatively homogeneous population of cells with larger nuclei, increased nuclear:cytoplasmic ratio, and no features of stratification and differentiation (Fig. 2, *C* and *D*). Multinucleate cells were again seen. The features in W12p24 and higher passages were similar to those of cervical SCC cell lines in monolayer culture (22, 23).

Histology of W12 in Organotypic Raft Culture. Progression of cell phenotype was also observed in organotypic raft cultures of W12. Consistent with previous findings (21), W12p9 (containing HPV16 episomes only) demonstrated a number of histological features of

low-grade SIL (Fig. 2*E*). The reconstituted epithelium showed mild basal atypia, with extensive surface differentiation and vacuolated cells reminiscent of koilocytes in the superficial layers. W12p14 (containing mixed episomes and integrants) showed greater nuclear crowding and atypia, which was present in the basal half of the epithelium (Fig. 2*F*). Some surface differentiation was retained, but this was reduced compared with W12p9, and dyskeratotic cells were present. The overall histological features of the epithelium were intermediate between those of W12p9 and W12p24. W12p24 and later passages (containing integrated HPV16 only) showed a higher grade of histological abnormalities (Fig. 2, *G* and *H*). Atypical basal-like cells were present throughout the epithelium, as were mitotic figures, many of which were abnormal (Fig. 2*H*). In addition, nests of cells extended irregularly into the underlying collagen matrix, suggesting that W12 had acquired an ability to invade collagen after integration of HPV16.

Ploidy. There was heterogeneity in ploidy levels at all passages of W12 analyzed (Fig. 3). W12p9 (episomes only) was predominantly near diploid, although approximately 20% of cells showed near tetraploid levels, consistent with nonselected endoreduplication events. In contrast, the majority of cells of W12p14 (mixed episomes and integrants) were near tetraploid, with no evidence of a biphasic population, indicating that after the commencement of HPV16 integration there was selection of cells that had undergone endoreduplication. W12 at higher passages was also predominantly tetraploid. In addition, we observed numerical abnormalities producing aneuploidy in a proportion of cells. These became detectable in W12p14 and increased in frequency with subsequent passages. The propensity for chromosome loss was greater than that for chromosome gain, and between passages 34 and 55, many cells were hypertriploid.

CNIs. CGH showed that the evolution of W12 in culture was associated with the gradual accumulation of CNIs, the majority of which were maintained in subsequent passages (Fig. 4). The number of CNIs in W12p55 was similar to that in the cervical SCC cell line SiHa. The majority of CNIs involved whole chromosomes or whole chromosome arms. Interestingly, copy number amplification of 5p was observed at W12p24 and higher passages and gain of 3q and loss of 3p were seen at W12p55. The variable gains seen on chromosomes 6 and 11 were shown by spectral karyotyping (Table 2) to be due to whole chromosome gains that were present in <50% cells and therefore at the limits of sensitivity of CGH, rather than being due to complex rearrangements.

Karyotype Analysis. Karyotypic heterogeneity was seen at each passage analyzed. To describe the most common karyotypic features at each passage, cells showing the most frequent ploidy level (*i.e.*, near diploid or near tetraploid) were used to generate a composite karyotype. The karyotypic features of W12 are illustrated in Fig. 5 and summarized in Table 2. By International System for Human Cytogenetic Nomenclature convention (34), only "clonal" chromosome aberrations are described in karyotype information. Clonal chromosome rearrangements and clonal chromosome gains represent those present in two or more metaphases analyzed, whereas clonal whole chromosome losses are those present in three or more metaphases analyzed. Where appropriate, data from CGH analysis were used to aid assignment of marker chromosomes.

Instability of Chromosome Number. Aneusomy was not observed in W12p9, which was diploid (Table 2). In contrast, in W12p14, which was near tetraploid, clonal numerical aberrations of nine chromosomes were detected. Several of these, such as gain of a single chromosome 20 and X, were maintained at high frequency on further passage. The clonal numerical aberrations seen from W12p14 onward varied between different passages (see Table 2), suggesting that loss and gain of chromosomes was a common event but that most of such aberrations did not confer a

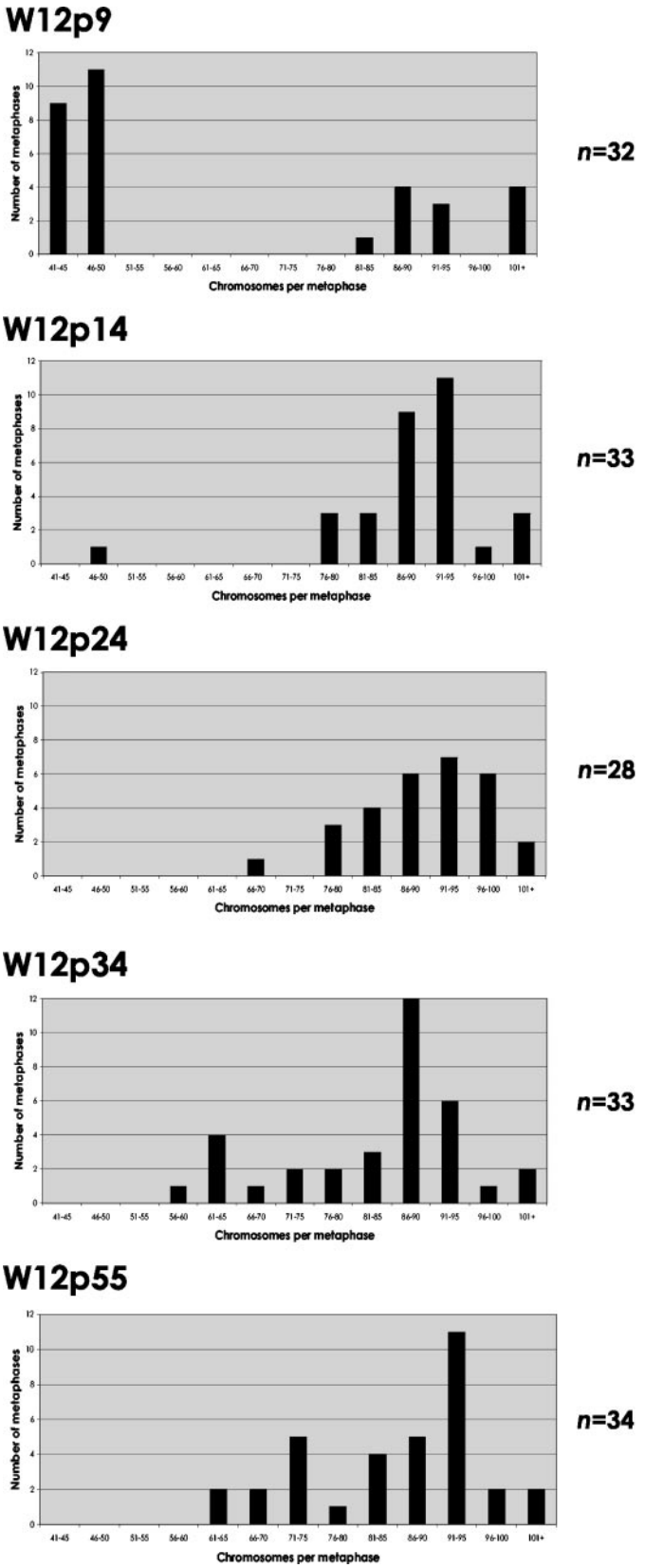

Fig. 3. Ploidy analysis of W12. Histograms demonstrating heterogeneity in ploidy of W12 at passages 9, 14, 24, 34, and 55. The number of metaphases analyzed (*n*) is indicated to the *right* of each histogram.

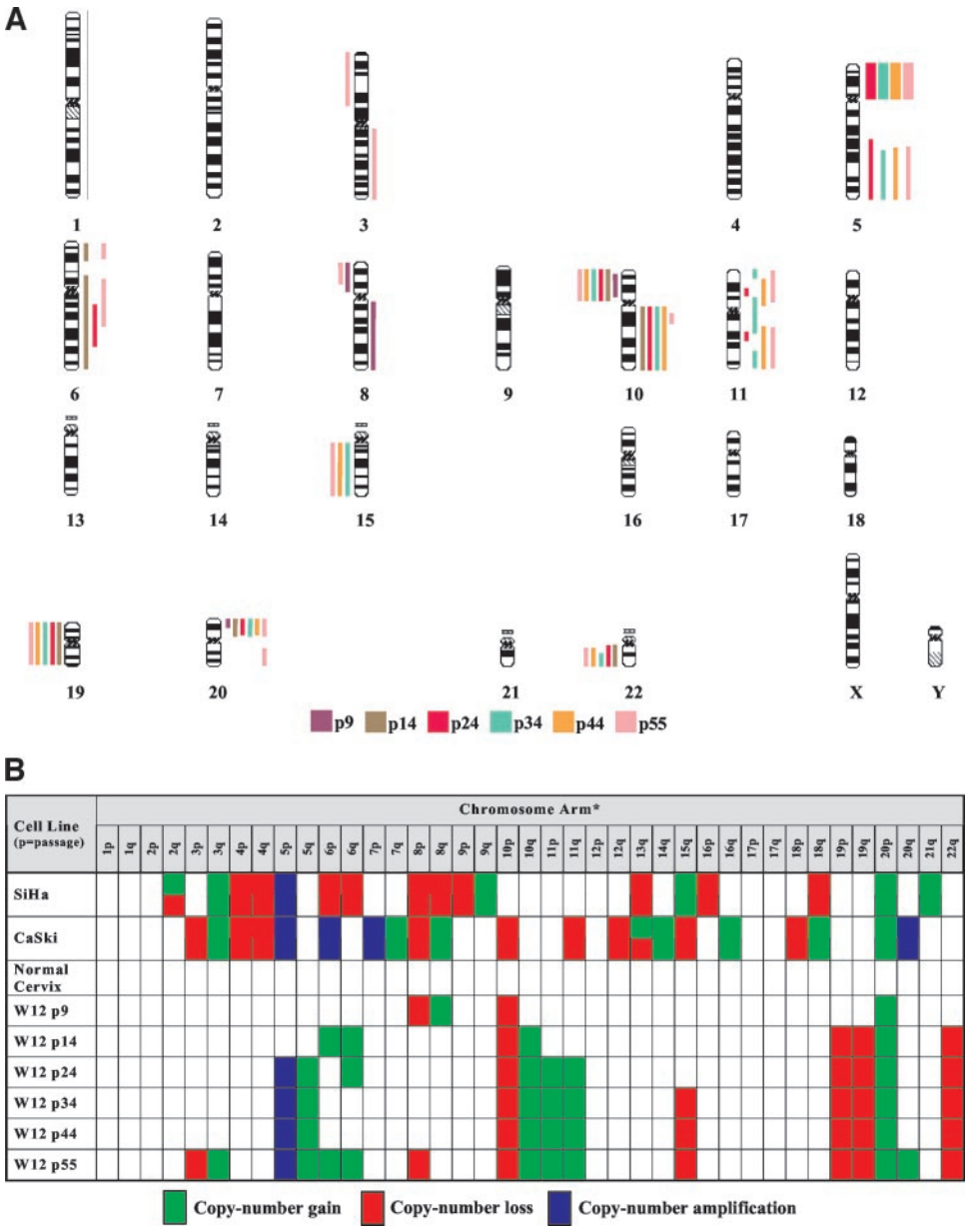

Fig. 4. Comparative genomic hybridization analysis of W12. *A*, sites of DNA copy number imbalances acquired by W12. *Vertical lines* to the *left* and *right* of the chromosome ideograms represent regions of genomic loss and gain, respectively, with *thicker vertical lines* representing high-level gain (amplification). *B*, patterns of accumulation of copy number imbalances on chromosome arms in W12. Data for the cervical SCC cell lines SiHa and CaSki and for normal ectocervical keratinocytes (normal cervix) are also shown.

selective advantage. Chromosomal loss became increasingly frequent between passage 24 and passage 55. Thus, the detection of numerical chromosomal instability in W12 coincided with the initial detection of integrated HPV16 genomes, when episomal genomes were also present. At this point, levels of HPV16 E7 protein were increased but had not attained maximal levels.

Instability of Chromosome Structure. In W12p9, only two chromosomal rearrangements, i(8q) and i(10q), were detected (Fig. 5*A*). Likewise, in W12p14, only two copies of the i(10q) were detected (Fig. 5*D*). Additional structural abnormalities were not observed until passage 24 onward, when only integrated HPV16 was present. Clonal structural aberrations present in W12p24 and maintained on further passage were a der(1)t(1;5) and a putative i(5p). This latter aberration correlated with the amplification of 5p seen by CGH in W12p24 and later passages (Fig. 4). Chromosome band-specific painting of W12p55 confirmed that the derivative was indeed an i(5p), present in two copies in most cells (Fig. 5*F*).

Additional clonal aberrations had also been acquired by passage 55 (Fig. 5*E*). A number of metaphases appeared to contain an i(3q) along with three normal copies of chromosome 3, consistent with CGH evidence of 3q gain and 3p loss, based on a tetraploid "baseline" (Fig. 4). A combination of whole chromosome painting and band-specific painting (Fig. 5*G*) was used to confirm that the i(3q) was present in W12p55, being detectable in 10 out of 10 metaphases analyzed.

In addition to the clonal marker chromosomes detected in two or more metaphases (and described in the W12 karyotypes), we also detected structural abnormalities that were present in single metaphases only (Table 2). We viewed these nonclonal rearrangements as also being indicative of chromosomal instability. They were detected only in W12p24 and higher passages. Detection of structural chromosomal instability therefore correlated with the selection of cells comprising only integrated HPV16 genomes, in which levels of the E7 protein were maximal.

DISCUSSION

Although integration of HR-HPV and acquisition of host genomic instability are key steps in cervical carcinogenesis (2, 9, 19), the lack

Table 2 *Chromosomal abnormalities acquired during progression of W12*

W12 passage	Ploidy[a]	Clonal whole chromosome gains[b]	Clonal whole chromosome losses[b]	Clonal chromosome rearrangements[b,c]	Nonclonal chromosome rearrangements
9	Near diploid			**i(8)(q10)**	
				i(10)(q10)	
		Composite karyotype:	45–46 ⟨2n⟩ ish wcp. XX, i(8)(q10) [7], i(10)(q10) [4] [cp7]		
14	Near tetraploid	+20	−22	**i(10)(q10)**	
		+6	−1		
		+16	−14		
		+X	−9		
		+5			
		Composite karyotype:	88–89 ⟨4n⟩ ish wcp. XXXX, +X [5], −1 [4], +5 [3], +6 [7], −9 [3], i(10)(q10)×2 [9], −14 [4], +16 [6], +20 [8], −22 [6] [cp9]		
24	Near tetraploid	+6	−19	**i(10)(q10)**	der(4)?
		+X	−22	**der(1)t(1;5)(p36;q21–22)**	der(15)?ins(18)
		+20		**i(5)(p10)**	der(16)?
		+11		der(X)del(X)(?p)del(X)(?q)	
		+5		der(3)del(3)(?p)del(3)(?q)	
		+16			
		+22			
		Composite karyotype:	86–100 ⟨4n⟩ ish wcp. XXXX, +X [8], der(X)del(X)(?p)del(X)(?q) [3], der(1)t(1;5)(p36;q21~22) [7], der(3)del(3)(?p)del(3)(?q) [3], +5 [5], +i(5)(p10)×2 [7], +6 [10], i(10)(q10)×2 [10], +11 [6], +16 [2], −19 [9], +20 [8], +22 [2], −22 [3] [cp11]		
34	Near tetraploid	+11	−19	**der(1)t(1;5)(p36;q21–22)**	der(?)t(1;3)
		+X	−15	**i(10)(q10)**	der(?)t(3;11)
		+20	−22	**i(5)(p10)**	der(?)t(8;10)
		+3	−10		der(?)t(6;8)
		+16	−4		der(?)t(10;15)
					der(?)t(12;18)
		Composite karyotype:	86–97 ⟨4n⟩ ish wcp. XXXX, +X [6], der(1)t(1;5)(p36;q21~22) [9], −4 [4], i(5)(q10) [2], +i(5)(p10)×2 [6], +i(5)(p10) [2], +6 [3], −10 [5], i(10)(q10)×2 [5], i(10)(q10) [4], +11 [7], −15 [6], +16 [2], −19 [9], +20 [4], −22 [6] [cp9]		
55	Near tetraploid	+X	−19	**der(1)t(1;5)(p36;q21–22)**	der(4)t(4;6)
		+20	−10	**i(5)(p10)**	der(?)t(10;15)
		+11	−13	**i(10)(q10)**	der(?)t(12;18)
		+6	−15	**i(3)(q10)**	
		+16	−7	?i(6)(p10)	
			−9	i(8)(q10)	
			−18	der(?)t(8;10)	
			−21		
			−22		
		Composite karyotype:	86–95 ⟨4n⟩ ish wcp. XXXX, +X [9], der(1)t(1;5)(p36;q21~22) [10], i(3)(q10) [5], +i(5)(p10)×2 [9], +6 [6], +?i(6)(p10) [4], −7 [4], i(8)(q10) [4], −10 [7], i(10)(q10) [7], +11 [7], −13 [6], −15 [6], +16 [4], −18 [4], −19 [10], +20 [8], −21 [3], −22 [3], der(?)t(8;10) [2] [cp10]		

[a] Karyotypic data for each passage were generated from metaphases with the most frequent ploidy level. See text for definition of clonal and nonclonal chromosome abnormalities
[b] Listed in order of decreasing frequency.
[c] Rearrangements in bold were present in >50% metaphases analyzed.

of a suitable biological reagent has hitherto prevented investigation of the precise temporal relationship between these events. The majority of HPV-infected cell lines have been generated by transfection of whole HR-HPV genomes. Although these lines acquire numerous genomic abnormalities (35–38), their inability to maintain HR-HPV genomes in episomal form precludes analysis of the relationship between integration and genomic instability. The W12 cell line was derived from a cervical low-grade SIL and acquired HPV16 through natural infection rather than transfection (21). W12 maintains episomes at low passage, but long-term cultivation *in vitro* leads to integration of HPV16 and complete loss of episomes (10). W12 therefore represents a unique model for investigating the association between integration of HPV16, the HPV type most commonly detected in cervical SCC (20), and acquisition of host cell genomic and phenotypic changes. In the present study, we have investigated genomic abnormalities acquired by W12 in monolayer culture, which selects for cells with a proliferative advantage. These conditions enable W12 to serve as a model of the effects of HPV16 infection in basal cervical squamous cells, the key site of deregulation of HR-HPV oncogenes in cervical neoplasia.

Our evidence that integration of HPV16 in W12 is associated with the emergence of cells showing gradually increasing levels of E7 protein and CFE is consistent with previous data (11). We have also demonstrated an increase in the histological grade of reconstituted epithelium formed by W12 in organotypic raft culture, with progression from a low-grade epithelium to a high-grade epithelium with microinvasive properties. The temporal associations between HPV16 physical state, E7 expression level, and host genomic changes in W12 are summarized in Fig. 6. When W12 contained only episomal HPV16, neither structural nor numerical chromosome instability was observed. Only low frequency endoreduplication of the host genome was seen. When integrated HPV16 was first detected (together with episomes) at p14, endoreduplicated genomes had been selected, and numerical chromosomal instability caused aneusomy to develop at high frequency. However, it was not until clones containing only integrated HPV16 emerged at passage 24 and higher passages that both numerical and structural chromosomal instability were observed. Thus, there was a close association between the physical state of HPV16 DNA and the presence and form of host cell genomic instability.

A likely cause of the genomic instability seen in W12 after integration is deregulated expression of the HPV16 oncoproteins E7 and E6. *In vitro*, overexpression of HR-HPV E7 and E6 from heterologous promoters can lead to ploidy changes and to numerical and structural chromosomal abnormalities (17, 18, 39, 40). An important strength of the W12 model is that during progression *in vitro*, E7 and E6 remain regulated by the homologous HPV16 promoter. Thus, W12 is likely to more accurately model the changes in HPV16 oncoprotein levels seen

Fig. 5. Spectral karyotyping and fluorescence *in situ* hybridization analysis of W12. *A*–*E*, spectral karyotyping classification karyograms of representative metaphases from W12p9, W12p14, and W12p55 are presented in *A*, *D*, and *E*, respectively. For W12p9, the inverted and contrast-enhanced 4′,6-diamidino-2-phenylindole image (*B*) and display color image (*C*) of the metaphase used to generate the classification karyogram are also shown. Structural aberrations are indicated by *white arrowheads*. *F*, band-specific painting of a representative W12p55 metaphase for 5p11–12 (*red*), 5p14 (*cyan*), and 5p15 (*green*), together with the average comparative genomic hybridization fluorescence ratio profile for chromosome 5 in W12p55. There are four copies of normal chromosome 5, as well as two copies of an i(5)(p10). *G*, painting of a representative metaphase from W12p55 for chromosome 3 (whole chromosome paint; *green*) and 3q21 (*orange*), together with the average comparative genomic hybridization fluorescence ratio profile for chromosome 3 in W12p55. There are three copies of a normal chromosome 3, as well as one copy of an i(3)(q10).

after integration *in vivo*. The elevated levels of E7 protein in W12 are attributable to deletion during integration of the 3′ region of the E2 ORF [which encodes the DNA-binding/dimerization domain required for transcriptional repression of the early promoter (41)], together with increased stability of virus-host transcripts using host poly(A) signals (42).

The forms of genomic instability that we observed in W12 were closely related to the levels of HPV16 E7 protein. Low levels of E7

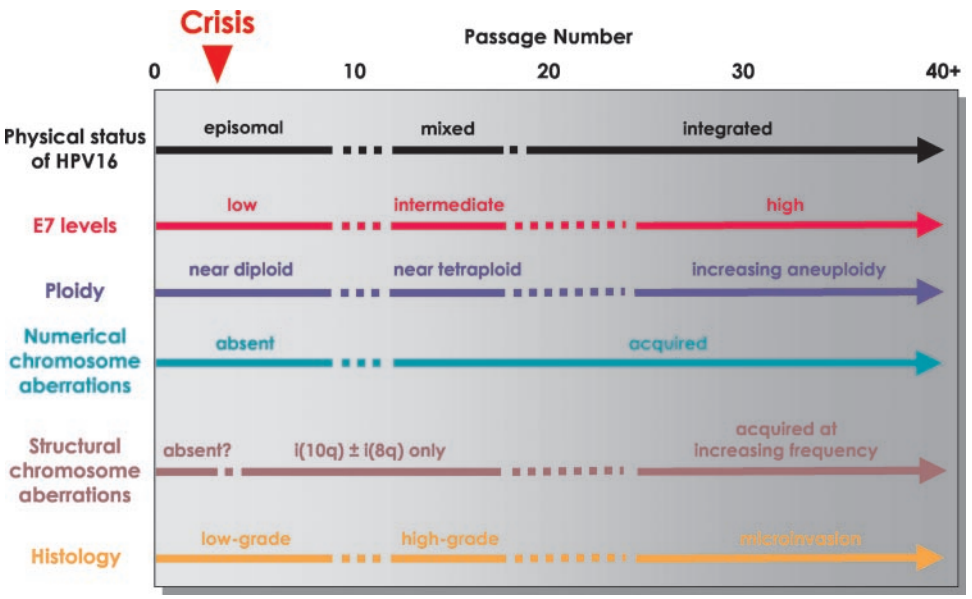

Fig. 6. Schematic representation of the temporal association between viral and genomic changes associated with long-term cultivation of W12. *Broken lines* illustrate that the precise timing of many viral/genomic changes could not be determined, given that not every passage of W12 was analyzed. The i(10q) and i(8q) present at the earliest passage analyzed were assumed to have arisen during a period of crisis at passage 3.

expressed from episomes were associated with a stable genome showing low frequency endoreduplication only. In contrast, higher levels of E7 were associated with the induction of aneusomy and maximal levels of E7 with the further acquisition of structural chromosomal abnormalities. The mechanisms underlying these changes are not certain. There is evidence that abnormalities in centrosome duplication caused by HPV16 E7 may lead to numerical chromosome instability (40). However, given that HR-HPV E6 and E7 bind multiple cellular proteins (4, 5), it is likely that there is functional abrogation of a large complement of host proteins when viral oncoprotein levels are high.

Although instability of chromosome structure was not observed in W12 until passage 24, it is interesting that two chromosomal rearrangements, an i(8q) and an i(10q), were detectable in W12p9, the earliest passage analyzed cytogenetically. These abnormalities were most likely acquired during a period of crisis in the establishment of W12 at around passage 3 (21). Consistent with this, we were able to detect high-level telomerase activity in all passages of W12 analyzed, including W12p9 (Table 1). A putative repressor of telomerase has previously been mapped to 10p (43), and rearrangements of chromosome 10, including i(10q) formation, are a frequent observation in HPV-immortalized cell lines (35, 44). Loss of chromosome 10p associated with i(10q) formation may therefore have been a necessary early event in activation of telomerase and immortalization of W12.

Our findings question the significance of polyploidy in the progression of carcinoma of the cervix. Tetraploid genomes were present at low frequency when only episomal HPV16 was detectable in W12p9, and they were not selected *in vitro*. Whereas tetraploidy was selected in W12p14, duplication of the copy of chromosome 5 into which HPV16 had integrated suggests that viral integration (with probable amplification of virus and flanking host sequences) preceded selection of the endoreduplicated genome. Selection of tetraploidy at passage 14 may therefore have been due to an increase in the effects of integrated HPV16 rather than to a selective advantage conferred by tetraploidy *per se*. The argument that polyploidy may not be of particular importance in cervical neoplastic progression is supported by some *in vivo* evidence, albeit from small studies, suggesting that it is aneuploidy rather than polyploidy that predicts progression of cervical SILs (45, 46).

Several aspects of our study reinforce the evidence (10, 21) that W12 is an accurate model of progression of HPV16-associated cervical neoplasia. Firstly, organotypic cultures demonstrated that the growth advantage acquired by W12 in monolayer culture after integration was associated with progression from a low-grade epithelium to a high-grade epithelium with microinvasive properties. Secondly, integration caused partial deletion of the E2 ORF, as is commonly observed *in vivo* and *in vitro* (11, 47), and occurred in the same chromosomal location as the common fragile site FRA5E, further supporting the evidence for preferential integration of HR-HPVs at or near common fragile sites (30, 32, 48). Thirdly, a number of the host genomic changes acquired by W12 during selection *in vitro* have also been described to occur during cervical carcinogenesis *in vivo*. For example, the gain of 3q and loss of 3p associated with i(3q) formation in W12p55 are two of the most frequent genomic CNIs observed in cervical SCCs and high-grade SILs (14, 15, 49). Similar considerations apply to the 5p amplification due to i(5p) formation, which was detected in W12p24 and subsequent passages and was associated with an ability to invade collagen. Cytogenetic studies have detected putative i(5p) derivative chromosomes in approximately 75% of cervical carcinomas and many SCC-derived cell lines (50, 51), and CGH has shown that amplification of 5p is associated with progression of SCC (15). Fourthly, the propensity toward chromosomal loss during progression of W12 is consistent with cytogenetic events that occur during the development of other tumor types (52). We conclude that the selection pressures encountered by W12 during passage *in vitro* lead to the acquisition of viral and host genomic changes that are similar or identical to those observed during cervical carcinogenesis *in vivo*.

It will now be important to assess whether the events that occur in W12 are also seen for other HPV types and in other cells of different genetic backgrounds. Other keratinocyte cell lines capable of maintaining HR-HPV episomes, such as the HPV31b-containing cell line CIN612 (53), will be of particular value in this regard. Cross-sectional studies of clinical samples of cervical SCC and SIL will also be of value to investigate the *in vivo* relationship among HPV type, HPV physical state, and host genomic abnormalities.

In summary, we have studied the unique cervical keratinocyte cell line W12, in which integration of HPV16 episomes occurs during *in vitro* passage and is associated with increasing levels of E7 protein as a result of deregulation of the homologous HPV16 promoter. We have shown that the acquisition of high-level genomic instability in cervical keratinocytes in monolayer culture only occurs after integration of HPV16. Different levels of E7 protein correlate with different forms of genomic instability, with only maximal E7 levels being associated with the acquisition of structural chromosomal abnormalities. Our data further emphasize the significance of integration of HR-HPV in cervical neoplastic progression *in vivo*. W12 represents an accurate model of cervical carcinogenesis and may prove to be a particularly valuable cell line for further investigation of the mechanisms and effects of HR-HPV integration in cervical keratinocytes.

ACKNOWLEDGMENTS

We thank Dawn Ward (Department of Pathology, University of Cambridge, Cambridge, United Kingdom) for assistance with tissue culture. We are also grateful to Dr. Paul Edwards (Department of Pathology, University of Cambridge) for help and advice with spectral karyotyping.

REFERENCES

1. Walboomers, J. M., Jacobs, M. V., Manos, M. M., Bosch, F. X., Kummer, J. A., Shah, K. V., Snijders, P. J., Peto, J., Meijer, C. J., and Munoz, N. Human papillomavirus is a necessary cause of invasive cervical cancer worldwide. J. Pathol., *189:* 12–19, 1999.
2. Arends, M. J., Buckley, C. H., and Wells, M. Aetiology, pathogenesis, and pathology of cervical neoplasia. J. Clin. Pathol., *51:* 96–103, 1998.
3. Schiffman, M. H., and Brinton, L. A. The epidemiology of cervical carcinogenesis. Cancer (Phila.), *76:* 1888–1901, 1995.
4. zur Hausen, H. Papillomaviruses causing cancer: evasion from host-cell control in early events in carcinogenesis. J. Natl. Cancer Inst. (Bethesda), *92:* 690–698, 2000.
5. Pim, D., Thomas, M., and Banks, L. The function of the human papillomavirus oncogenes. *In:* R. J. A. Grand (ed.), Viruses, Cell Transformation and Cancer, Vol. 5, pp. 145–192. Amsterdam: Elsevier Science, 2001.
6. Higgins, G. D., Uzelin, D. M., Phillips, G. E., McEvoy, P., Marin, R., and Burrell, C. J. Transcription patterns of human papillomavirus type 16 in genital intraepithelial neoplasia: evidence for promoter usage within the E7 open reading frame during epithelial differentiation. J. Gen. Virol., *73:* 2047–2057, 1992.
7. Durst, M., Glitz, D., Schneider, A., and zur Hausen, H. Human papillomavirus type 16 (HPV 16) gene expression and DNA replication in cervical neoplasia: analysis by *in situ* hybridization. Virology, *189:* 132–140, 1992.
8. Zhao, W., Chow, L. T., and Broker, T. R. Transcription activities of human papillomavirus type 11 E6 promoter-proximal elements in raft and submerged cultures of foreskin keratinocytes. J. Virol., *71:* 8832–8840, 1997.
9. Lazo, P. A. The molecular genetics of cervical carcinoma. Br. J. Cancer, *80:* 2008–2018, 1999.
10. Alazawi, W., Pett, M., Arch, B., Scott, L., Freeman, T., Stanley, M. A., and Coleman, N. Changes in cervical keratinocyte gene expression associated with integration of human papillomavirus 16. Cancer Res., *62:* 6959–6965, 2002.
11. Jeon, S., Allen-Hoffman, B. L., and Lambert, P. F. Integration of human papillomavirus type 16 into the human genome correlates with a selective growth advantage of cells. J. Virol., *69:* 2989–2997, 1995.
12. Klaes, R., Woerner, S. M., Ridder, R., Wentzensen, N., Duerst, M., Schneider, A., Lotz, B., Melsheimer, P., and von Knebel Doeberitz, M. Detection of high-risk cervical intraepithelial neoplasia and cervical cancer by amplification of transcripts derived from integrated papillomavirus oncogenes. Cancer Res., *59:* 6132–6136, 1999.

13. Kirkland, J., Stanley, M. A., and Cellier, K. A comparative study of histological and chromosomal abnormalities in cervical carcinoma. Cancer (Phila.), *20:* 1934–1952, 1967.
14. Heselmeyer, K., Schrock, E., du Manoir, S., Blegen, H., Shah, K., Steinbeck, R., Auer, G., and Ried, T. Gain of chromosome 3q defines the transition from severe dysplasia to invasive carcinoma of the uterine cervix. Proc. Natl. Acad. Sci. USA, *93:* 479–484, 1996.
15. Heselmeyer, K., Macville, M., Schrock, E., Blegen, H., Hellstrom, A. C., Shah, K., Auer, G., and Ried, T. Advanced-stage cervical carcinomas are defined by a recurrent pattern of chromosomal aberrations revealing high genetic instability and a consistent gain of chromosome arm 3q. Genes Chromosomes Cancer, *19:* 233–240, 1997.
16. Ried, T., Heselmeyer-Haddad, K., Blegen, H., Schrock, E., and Auer, G. Genomic changes defining the genesis, progression, and malignancy potential in solid human tumors: a phenotype/genotype correlation. Genes Chromosomes Cancer, *25:* 195–204, 1999.
17. White, A. E., Livanos, E. M., and Tlsty, T. D. Differential disruption of genomic integrity and cell cycle regulation in normal human fibroblasts by the HPV oncoproteins. Genes Dev., *8:* 666–677, 1994.
18. Duensing, S., and Munger, K. The human papillomavirus type 16 E6 and E7 oncoproteins independently induce numerical and structural chromosome instability. Cancer Res., *62:* 7075–7082, 2002.
19. Stanley, M. A. Human papillomavirus and cervical carcinogenesis. Best Pract. Res. Clin. Obstet. Gynaecol., *15:* 663–676, 2001.
20. Bosch, F. X., Manos, M. M., Munoz, N., Sherman, M., Jansen, A. M., Peto, J., Schiffman, M. H., Moreno, V., Kurman, R., and Shah, K. V. Prevalence of human papillomavirus in cervical cancer: a worldwide perspective. International Biological Study on Cervical Cancer (IBSCC) Study Group. J. Natl. Cancer Inst. (Bethesda), *87:* 796–802, 1995.
21. Stanley, M. A., Browne, H. M., Appleby, M., and Minson, A. C. Properties of a non-tumorigenic human cervical keratinocyte cell line. Int. J. Cancer, *43:* 672–676, 1989.
22. Friedl, F., Kimura, I., Osato, T., and Ito, Y. Studies on a new human cell line (SiHa) derived from carcinoma of uterus. I. Its establishment and morphology. Proc. Soc. Exp. Biol. Med., *135:* 543–545, 1970.
23. Pattillo, R. A., Hussa, R. O., Story, M. T., Ruckert, A. C., Shalaby, M. R., and Mattingly, R. F. Tumor antigen and human chorionic gonadotropin in CaSki cells: a new epidermoid cervical cancer cell line. Science (Wash. DC), *196:* 1456–1458, 1977.
24. Coleman, N., Greenfield, I. M., Hare, J., Kruger-Gray, H., Chain, B. M., and Stanley, M. A. Characterization and functional analysis of the expression of intercellular adhesion molecule-1 in human papillomavirus-related disease of cervical keratinocytes. Am. J. Pathol., *143:* 355–367, 1993.
25. Roberts, I., Wienberg, J., Nacheva, E., Grace, C., Griffin, D., and Coleman, N. Novel method for the production of multiple colour chromosome paints for use in karyotyping by fluorescence *in situ* hybridisation. Genes Chromosomes Cancer, *25:* 241–250, 1999.
26. Freshney, R. I. Quantitation. *In:* Culture of Animal Cells: A Manual of Basic Technique, 4th ed., pp. 309–328. New York: Wiley-Liss, 2000.
27. Kinjo, T., Kamiyama, K., Chinen, K., Iwamasa, T., Kurihara, K., and Hamada, T. Squamous metaplasia induced by transfection of human papillomavirus DNA into cultured adenocarcinoma cells. Mol. Pathol., *56:* 97–108, 2003.
28. Liu, Y., You, H., Chiriva-Internati, M., Korourian, S., Lowery, C. L., Carey, M. J., Smith, C. V., and Hermonat, P. L. Display of complete life cycle of human papillomavirus type 16 in cultured placental trophoblasts. Virology, *290:* 99–105, 2001.
29. Sarkar, G., Turner, R. T., and Bolander, M. E. Restriction-site PCR: a direct method of unknown sequence retrieval adjacent to a known locus by using universal primers. PCR Methods Appl., *2:* 318–322, 1993.
30. Thorland, E. C., Myers, S. L., Persing, D. H., Sarkar, G., McGovern, R. M., Gostout, B. S., and Smith, D. I. Human papillomavirus type 16 integrations in cervical tumors frequently occur in common fragile sites. Cancer Res., *60:* 5916–5921, 2000.
31. Shing, D. C., Morley-Jacob, C. A., Roberts, I., Nacheva, E., and Coleman, N. Ewing's tumour: novel recurrent chromosomal abnormalities demonstrated by molecular cytogenetic analysis of seven cell lines and one primary culture. Cytogenet. Genome Res., *97:* 20–27, 2002.
32. Thorland, E. C., Myers, S. L., Gostout, B. S., and Smith, D. I. Common fragile sites are preferential targets for HPV16 integrations in cervical tumors. Oncogene, *22:* 1225–1237, 2003.
33. Stanley, M. A., and Greenfield, I. M. Culture of human cervical epithelial cells. *In:* Culture of Epithelial Cells, R. I. Freshney and M. G. Freshney (eds.), pp. 135–158. New York: Wiley-Liss, 1992.
34. Mitelman, F. ISCN 1995: An International System for Human Cytogenetic Nomenclature (1995). Memphis, TN: Karger Publishers Inc., 1995.
35. Cottage, A., Dowen, S., Roberts, I., Pett, M., Coleman, N., and Stanley, M. Early genetic events in HPV immortalised keratinocytes. Genes Chromosomes Cancer, *30:* 72–79, 2001.
36. Solinas-Toldo, S., Durst, M., and Lichter, P. Specific chromosomal imbalances in human papillomavirus-transfected cells during progression toward immortality. Proc. Natl. Acad. Sci. USA, *94:* 3854–3859, 1997.
37. Smith, P. P., Bryant, E. M., Kaur, P., and McDougall, J. K. Cytogenetic analysis of eight human papillomavirus immortalized human keratinocyte cell lines. Int. J. Cancer, *44:* 1124–1131, 1989.
38. Steenbergen, R. D., Walboomers, J. M., Meijer, C. J., van der Raaij-Helmer, E. M., Parker, J. N., Chow, L. T., Broker, T. R., and Snijders, P. J. Transition of human papillomavirus type 16 and 18 transfected human foreskin keratinocytes towards immortality: activation of telomerase and allele losses at 3p, 10p, 11q and/or 18q. Oncogene, *13:* 1249–1257, 1996.
39. Southern, S. A., Noya, F., Meyers, C., Broker, T. R., Chow, L. T., and Herrington, C. S. Tetrasomy is induced by human papillomavirus type 18 E7 gene expression in keratinocyte raft cultures. Cancer Res., *61:* 4858–4863, 2001.
40. Duensing, S., Duensing, A., Crum, C. P., and Munger, K. Human papillomavirus type 16 E7 oncoprotein-induced abnormal centrosome synthesis is an early event in the evolving malignant phenotype. Cancer Res., *61:* 2356–2360, 2001.
41. Howley, P. M. Papillomavirinae: the viruses and their replication. *In:* B. N. Fields, D. M. Knipe, and P. M. Howley (eds.), Fundamental Virology, 3rd ed., pp. 947–948. Philadelphia: Lippincott-Raven, 1996.
42. Jeon, S., and Lambert, P. F. Integration of human papillomavirus type 16 DNA into the human genome leads to increased stability of E6 and E7 mRNAs: implications for cervical carcinogenesis. Proc. Natl. Acad. Sci. USA, *92:* 1654–1658, 1995.
43. Nishimoto, A., Miura, N., Horikawa, I., Kugoh, H., Murakami, Y., Hirohashi, S., Kawasaki, H., Gazdar, A. F., Shay, J. W., Barrett, J. C., and Oshimura, M. Functional evidence for a telomerase repressor gene on human chromosome 10p15.1. Oncogene, *20:* 828–835, 2001.
44. Pei, X. F., Meck, J. M., Greenhalgh, D., and Schlegel, R. Cotransfection of HPV-18 and v-fos DNA induces tumorigenicity of primary human keratinocytes. Virology, *196:* 855–860, 1993.
45. Bibbo, M., Dytch, H. E., Alenghat, E., Bartels, P. H., and Wied, G. L. DNA ploidy profiles as prognostic indicators in CIN lesions. Am. J. Clin. Pathol., *92:* 261–265, 1989.
46. Kashyap, V., and Das, B. C. DNA aneuploidy and infection of human papillomavirus type 16 in preneoplastic lesions of the uterine cervix: correlation with progression to malignancy. Cancer Lett., *123:* 47–52, 1998.
47. Choo, K. B., Pan, C. C., and Han, S. H. Integration of human papillomavirus type 16 into cellular DNA of cervical carcinoma: preferential deletion of the E2 gene and invariable retention of the long control region and the E6/E7 open reading frames. Virology, *161:* 259–261, 1987.
48. Wentzensen, N., Ridder, R., Klaes, R., Vinokurova, S., Schaefer, U., and Doeberitz, M. K. Characterization of viral-cellular fusion transcripts in a large series of HPV16 and 18 positive anogenital lesions. Oncogene, *21:* 419–426, 2002.
49. Kirchhoff, M., Rose, H., Petersen, B. L., Maahr, J., Gerdes, T., Lundsteen, C., Bryndorf, T., Kryger-Baggesen, N., Christensen, L., Engelholm, S. A., and Philip, J. Comparative genomic hybridization reveals a recurrent pattern of chromosomal aberrations in severe dysplasia/carcinoma *in situ* of the cervix and in advanced-stage cervical carcinoma. Genes Chromosomes Cancer, *24:* 144–150, 1999.
50. Dowen, S. E., Neutze, D. M., Pett, M. R., Cottage, A., Stern, P., Coleman, N., and Stanley, M. A. Amplification of chromosome 5p correlates with increased expression of Skp2 in HPV-immortalized keratinocytes. Oncogene, *22:* 2531–2540, 2003.
51. Atkin, N. B., and Baker, M. C. Small metacentric marker chromosomes in unbanded archival material from carcinomas of the cervix uteri. Cytobios., *65:* 179–185, 1991.
52. Dutrillaux, B. Pathways of chromosome alteration in human epithelial cancers. Adv. Cancer Res., *67:* 59–82, 1995.
53. Bedell, M. A., Hudson, J. B., Golub, T. R., Turyk, M. E., Hosken, M., Wilbanks, G. D., and Laimins, L. A. Amplification of human papillomavirus genomes *in vitro* is dependent on epithelial differentiation. J. Virol., *65:* 2254–2260, 1991.

Acquisition of High-Level Chromosomal Instability Is Associated with Integration of Human Papillomavirus Type 16 in Cervical Keratinocytes

Mark R. Pett, William O. F. Alazawi, Ian Roberts, et al.

Cancer Res 2004;64:1359-1368.